# Lab on a Chip

Accepted Manuscript






ROYAL SOCIETY OF CHEMISTRY

www.rsc.org/loc

Lab on a Chip

CRITICAL REVIEW

# Microfluidic devices to enrich and isolate circulating tumor cells

J. H. Myung[a] and S. Hong[a, b]*

Received 00th January 20xx,
Accepted 00th January 20xx

DOI: 10.1039/x0xx00000x

www.rsc.org/

Given the potential clinical impact of circulating tumor cells (CTCs) in blood as a clinical biomarker for diagnosis and prognosis of various cancers, a myriad of detection methods for CTCs have been recently introduced. Among those, a series of microfluidic devices are particularly promising as these uniquely offer micro-scale analytical systems that are highlighted by low consumption of samples and reagents, high flexibility to accommodate other cutting-edge technologies, precise and well-defined flow behaviors, and automation capability, presenting significant advantages over the conventional larger scale systems. In this review, we highlight the advantages of microfluidic devices and the translational potential into CTC detection methods, categorized by miniaturization of bench-top analytical instruments, integration capability with nanotechnologies, and *in situ* or sequential analysis of captured CTCs. This review provides a comprehensive overview of recent advances in the CTC detection achieved through application of microfluidic devices and their challenges that these promising technologies must overcome to be clinically impactful.

## 1. Introduction

Circulating tumor cells (CTCs) in cancer patient blood have shown promise as a clinical biomarker for cancer diagnosis, prognosis, prediction, stratification, and pharmacodynamics without invasive tissue biopsy.[1-3] According to 'seed and soil theory',[4] CTCs escaped from the primary tumor sites travel through the bloodstream until either extravasating and initiating secondary tumor colonies or dying. Over the past decade, a number of technologies have been developed to discriminate CTCs based on their biological and/or physiochemical properties that are distinct from normal hematological cells.[5, 6] Among those, CellSearch® and Gilupi, approved by US FDA and EU, respectively, are in advanced stages of clinical translation. CellSearch® (Janssen Diagnostics), the semi-automated CTC detection system approved for breast, prostate, and colorectal metastatic cancers, relies on the immunomagnetic separation of CTCs using an antibody against a CTC marker, epithelial cell adhesion molecule (EpCAM).[1] Gilupi is an *in vivo* CTC isolation system for CTC quantification and post-capture analysis *ex vivo* via insertion of a CellCollector tip functionalized with polymers and anti-EpCAM into blood vessel.[7] However, the rarity (approximately one CTC in the background of $10^6$-$10^9$ hematologic cells), epithelial-mesenchymal plasticity, and heterogeneity of CTCs have hampered clinically reliable detection and molecular characterization of CTCs.[8, 9]

A variety of the emerging microfluidic devices have introduced several important advantages and enhancement to existing CTC capture strategies, including size-based separation, dielectrophoresis-based separation, immunoaffinity-based capture, fluorescence-based sorting, and immunomagnetic capture of CTCs, as comprehensively reviewed earlier by others.[10-16] Many kinds of materials, such as polymers (e.g. polydimethylsiloxane (PDMS)), ceramics (e.g. glass), semi-conductors (e.g. silicon) and metals, have been used to develop microfluidic devices for CTC capture. Among those, due to its optical characteristics, biological and chemical compatibility, fast prototyping, and cost-efficiency,[17] PDMS allows for microfluidic devices to be easily fabricated using standard photolithography and integrated with other nanotechnologies. As a result, PDMS has been most commonly used for microfluidic devices for detection and isolation of CTCs particularly in their early development stages.[18] Although highly promising, for those microfluidic devices to be successfully translated, several limitations, such as batch-to-batch variations, slow processing speed of rare cells in large sample volume, and non-specific binding, must be overcome.[19]

In this review, we focus on how the advantages of microfluidic devices have been exploited to enhance CTC enrichment and detection. The advantages of microfluidic devices and their recent examples are summarized in **Table 1**. The recent microfluidic device techniques implemented to CTC devices are classified into one of the three principal approaches based on the roles of microfluidic technology played in CTC enrichment and detection: (i) miniaturization of conventional bench-top instruments for cell sorting; (ii) integration with nanotechnologies for improved performance; and (iii) enabling *in situ* post-capture analysis. Within each category, several subsections are also provided to further categorize each technology based on its detection/functional mechanisms. In

[a] 833 S. Wood St., Department of Biopharmaceutical Sciences, College of Pharmacy, University of Illinois, Chicago, IL, 60612.
[b] Division of Integrated Science and Engineering and Department of Integrated OMICs for Biomedical Sciences, Yonsei University, Seoul, KOREA 03706.

**Table 1**. The advantages of microfluidic devices for enhancing CTC enrichment and detection, and their related recent examples.

| Advantages | Related properties | Applications | Examples |
|---|---|---|---|
| Miniaturization of conventional, bench-top instrument for cell sorting | • Small amount of sample and reagents required<br>• Well-controlled fluidic behaviour<br>• Easy to design, modify, and fabricate the devices<br>• Transparent, soft, and flexible | • Microfilters for size-based separation<br>• Micro-centrifuge for density-based separation<br>• Micro-immunoassay<br>• Micro-MACS<br>• Micro-FACS | Ref 22 - 31<br>Ref 33, 34<br>Ref 37, 38<br>Ref 39 - 45<br>Ref 46, 47 |
| Integration capability with other nanotechnology | • Surface functionalization using silane chemicals<br>• Transparent, soft, and flexible | • Integration with nanostructured surface<br>• Combination with magnetic beads<br>• Integration with polymers to enhance CTC capture and release efficiencies | Ref 55 - 57<br>Ref 58, 59<br>Ref 66 - 70 |
| *in situ* post-capture analysis | • High gas permeability (especially to $CO_2$ than to $O_2$)<br>• Transparent, soft, and flexible | • *in situ* analysis<br>• Sequential analysis after release the cells | Ref 75, 76<br>Ref 74, 78 |

addition, we discuss key challenges that the microfluidic CTC devices encounter, which should be overcome for this promising technology to be clinically impactful.

## 2. Roles of microfluidics in CTC enrichment and detection

Microfluidic technology can be considered both as a study of fluidic behaviors in micro-channels and a manufacturing method of microfluidic devices. A microfluidic device typically manipulates small amounts ($10^{-6}$ to $10^{-12}$ L) of fluid using 1 to 1,000 μm channel sizes. Microfluidic systems with small sample volumes, multiplexing capabilities, and large surface-area-to-volume ratios offer a unique way for capture and detection of rare CTCs. Specifically, the microfluidic devices enable: i) the use of very small quantities of samples and reagents to carry out highly sensitive detection; ii) facile integration with other technologies that improve the efficiency of the device; and iii) a one-step process of sample loading, separation, and analysis.

### 2.1. Miniaturization

Microfluidic devices are originally designed for miniaturization for chemistry, physics, biology, materials science, and bioengineering from mm-scale to μm-scale. The majority of the conventional CTC detection methods are designed as bench-top instruments, such as magnetic-activated cell sorter (MACS), fluorescence-activated cell sorter (FACS), high-definition fluorescence scanning microscopy, isolation by size of epithelial tumor cells (ISET), and density-gradient cell sorting using a centrifuge. Microfluidic systems have been recently developed to provide miniature structure and integrated processing capability by down-scaling such bench-top instruments.[20, 21] Compared to bench-top instruments, the CTC microfluidic devices require only a small amount of reagents, enable to achieve superior sensitivity, and enhance enrichment on the small surface area. As a result, the CTC microfluidic devices enable cost-effective, simple, and automated operation, along with precise control over the flow behaviors and biological interactions of CTCs in the microchannel.[20, 14]

**2.1.1. Microfilters for size-based separation** Based on the morphological and size differences between cancer cells (15–40 μm in diameter) and leukocytes (≤10 μm in diameter), size-based filtration using either polymer membranes or microsieve membrane filter devices made of silicon or nickle have been shown to extract CTCs from whole blood samples.[22-26] The size, geometry, and density of the pores in the microfilters can be uniformly and precisely controlled.[23] With batch fabrication, this technology can also afford maximal sample processing capability through parallel arrays of multiple flow cells, which reduces processing time, cost, and filter clogging, while facilitating mass production and high-throughput screening for large-scale clinical studies.[26] A silicon microsieve device with a high-density pore array was able to rapidly filter tumor cells from whole blood.[24] The highly porous structure (~5,000 pores with 10 μm in diameter per $mm^2$) of a thin silicon membrane (30 μm in thickness, $10^5$ pores per device) minimized the fluid resistance, allowing rapid CTC filtration at a high flow rate of 1 mL $min^{-1}$ (**Fig. 1a-1c**). From cancer cell-spiked human whole blood, more than 80% of MCF-7 and HepG2 cells were recovered at a rapid flow rate of 1 mL $min^{-1}$. The device was further validated with blood from cancer patients. The whole process, from loading of blood samples drawn from various cancer patients (8 samples) to CTC count, was completed in 1.5 h. In addition, the rigid silicon structure and small device footprint (5 mm in diameter) allowed *in situ* immunostaining for CTC identification directly on the microsieves. However, considering that the size of most CTCs in clinical samples widely varies and is often found to be similar to that of leukocytes, as opposed to that of *in vitro* cancer cell lines,[27, 28] these size-based microfiltration systems for CTC detection require further validation with clinical samples.

It is noteworthy that it has been reported that CTCs that form clusters are more invasive and metastatic than CTCs that are present in their single cell form.[29, 30] As a result, methods to isolate the CTC clusters from blood have been developed.[30, 31] For example, Cluster-Chip utilizes a microfluidic device



 

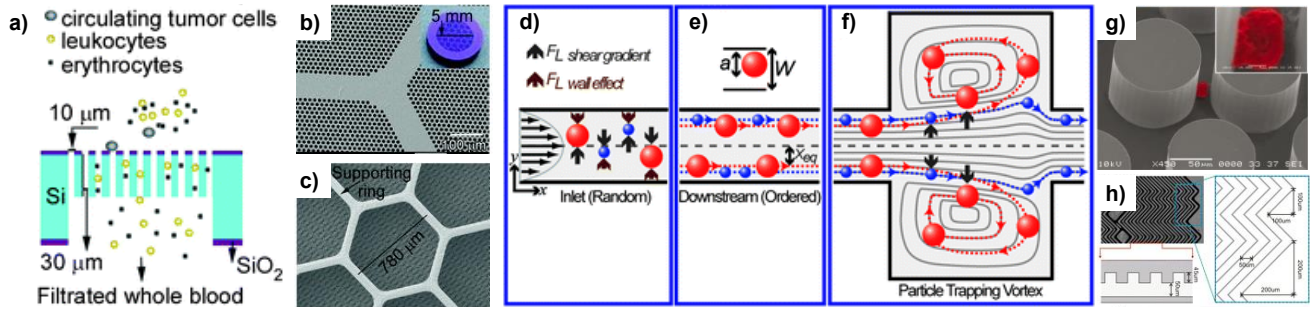


**Fig. 1**. Miniaturization of a filter, a centrifuge, and an immunoassay for CTC detection. (a) A schematic illustration of size-based CTC separation using a silicon microsieve. The diameter of the fabricated microsive is around 5 mm in diameter (b), which includes micropores of 10 μm in diameter and a supporting ring as shown in the SEM image (c). The fabricated microfilter is sandwiched between the microscope plate and the blood reservoir, and whole blood was injected into the microsieve filter using a peristaltic pump. (Reproduced by permission of Royal Society of Chemistry) (d-f) A scheme of the separation mechanism of cells with different densities in a microcentrifuge. After being injected into the microchannels, the cell mixtures were subjected to a shear gradient lift force, which directs particles toward the channel wall, and a wall effect lift force, directed toward the channel center (d). The balance between the shear gradient and the wall effect lift forces near dynamic equilibrium positions (e), $X_{eq}$, was broken when the lift forces were decoupled near the particle trapping chamber (f), and CTCs were separated from blood cells. (Reproduced by permission of Royal Society of Chemistry) (g and h) The miniaturized immunoassay, CTC-chip with a micropost array (1st generation, g) and herringbone patterns (2nd generation, h) were able to capture CTCs from whole blood after being functionalized with anti-EpCAM on the silicon (g) or PDMS (h) surface, for point-of-care isolation of CTCs from peripheral blood. (Reproduced by permission of Nature Publishing Group (g) and National Academy of Sciences (h))

integrated with specialized bifurcating traps.[31] The PDMS–based microfluidic devices consisted of 4,096 parallel tracks, and each CTC-cluster trap was comprised of multiple rows of shifted triangular pillars.[31] Their preliminary data using MDA-MB-231 cell cluster-spiked human blood revealed that the Cluster-Chip showed higher capture efficiency (near 100%) at 2.5 mL $h^{-1}$, in a direct comparison with 5 μm membrane filters (only ~26% at 0.1 psi). Because this Cluster-Chip is immunolabeling-independent and composed of shifted triangular pillars, 80% of the captured CTC clusters were released from the Cluster-Chip by simply reversing the flow and transiently cooling the samples to 4°C. The captured CTC clusters from blood of breast cancer, melanoma, or prostate cancer patients were also used for subsequent RNA sequencing and immunostaining, which showed low expression levels of transcripts encoding CTC markers, such as keratins, MUC1, EpCAM, or CDH1.[31]

**2.1.2. micro-Centrifuge** Based on the distinct size and density differences between cancer cells and leukocytes, the miniaturized micro-centrifuge, or centrifuge-on-a-chip, can also isolate CTCs from whole blood samples.[32] Typical bench-top centrifuges are widely used for separation of cells by size/density particularly during sample preparation. The micro-centrifuge with a μL-scale channel volume can replicate the functions of a conventional centrifuge simply relying on a purely fluid dynamics phenomenon.[32] The well-controlled flow behaviors in microchannels selectively separate and trap CTCs in microscale vortices without moving parts or external forces. Because of its high parallel processing capability, this technology can also shorten processing time, reduce cost and filter clogging, and provide high-throughput screening for clinical studies.[32, 33]

A micro-centrifuge with laminar fluid microvortices have been demonstrated to continuously trap and enrich cancer cells from spiked blood samples using hydrodynamic forces.[33] At a speed of 5 mL $min^{-1}$, a balance and decoupling of a shear gradient lift force and a wall effect lift force in laminar vortices and microvortex chambers induced the particle entry and trapping within the microvortex chambers, as depicted in **Fig. 1c-1e**. Without the need for manual pipetting and washing steps, the micro-centrifuge was reported to enrich rare cancer cells from blood samples with minimal cytotoxicity (~90% of cell viability). The capability of on-chip fluorescence labeling of intra- and extra-cellular antigens also enabled to identify and quantify the trapped cancer cells (~40% capture purity). This simple micro-centrifuge could be potentially used to develop an automated, low-cost, and high-throughput system for CTC enrichment as an alternative to the standard bench-top centrifuge in standardized clinical diagnostics or resource-poor settings.[34]

**2.1.3. Miniaturized immunoassay** Conventional immunoarray systems, such as the enzyme-linked immunosorbent assay (ELISA), can be integrated with portable microfluidic devices. The immunoassay is one of the main analytical techniques used in biomedical applications due to the highly sensitive and selective binding properties of antigen–antibody interaction, allowing for specific analyte detection.[35] However, conventional immunoassays require a labor-intensive process of multiple reagents treatment/incubation and several washing steps. To address this issue, the conventional immunoassay has been miniaturized on microfluidic devices to control binding kinetics, reduce reagent consumption, and automate the process with precise control.[35, 36] The surface of a PDMS microfluidic device can be functionalized with silane chemicals to immobilize proteins, polymers, and inorganic materials (more details in Section 2.2).[5, 6] Compared to immune-free detection methods using microfilters and micro-centrifuge described in the previous sections, an immunoarray, similar to micro-MACS and micro-FACS described in later

sections, requires specific antibodies against surface markers on target cells. EpCAM has been most commonly used as a capture agent in these devices because its overexpression on various CTCs with epithelial origin but no expression by normal hematologic cells.

CTC capture efficiency of the microfluidic immunoassay devices can be further enhanced by modifying hydrodynamic mixing efficiency in the microfluidic devices. The Toner/Haber group has developed a microfluidic device called CTC-chip, which is in its advanced stage of development (**Fig. 1f and 1g**).[37, 38] The CTC-chip showed great potential for simple and cost-effective CTC detection. The silicon (the 1st generation) and PDMS (the 2nd generation) chip surfaces were modified using a series of chemicals, i.e., 3-mercaptopropyo trimethoxysilane (MPTMS), N-y-maleimidobutyryloxy succinimide ester (GMBS), NeutrAvidin, and biotinylated anti-EpCAM. Microposts incorporated into the fluidic channels (the 1st generation) enhanced the hydrodynamic efficiency of the flow, resulting in sensitive detection of CTCs under flow.[37] Although the micropost-based system exhibited a high capture yield at a low flow rate (1-2 mL per hour), the capture yield substantially decreased with an increase in flow rate (higher than 2.5 mL $hr^{-1}$) due to the insufficient time for CTCs to bind to the surface. It has been also reported that the first generation of CTC chip showed poor mixing efficiency of viscous flow due to low diffusivity. In an effort of addressing these issues, subsequent studies have incorporated herringbone patterns on the ceiling of the 2nd generation microfluidic device, increasing the mixing efficiency.[38] Modifications onto the microchannel surfaces, such as microposts and 2-dimensional grooves, have been shown to be effective in increasing contact surface area and disrupting laminar flow to maximize collisions between CTCs and antibody-coated surface, enhancing overall CTC capture efficiency.[38] However, these modifications could cause non-specific capture or clogging of CTC clusters[38] at the regions where flow is locally rotating or local shear stress is low.

**2.1.4. micro-MACS** CTC detection using micro-MACS is one of the most widely used approaches. Compared to conventional bench-top MACS, a downscaled microfluidic system provides a well-confined flow and magnetic field because its short vertical height and large cross-section help to increase the sensitivity of the magnetic capture.[21] Similar to the conventional MACS system for CellSearch®, a microfluidic-based immunomagnetic assay uses antibody-conjugated magnetic beads and an external magnetic field for capturing. However, one unique difference of micro-MACS is that, depending on the direction of the magnetic field, the collection location of the target cell can be controlled (inside or outside of the microfluidic devices). For example, a device reported by the Ingber lab retained the captured CTCs on the chip for *in situ* post-capture analysis.[39] It has also been reported that magnetically driven collection of CTCs can be controlled to be located at different outlets.[40] Although the potential cytotoxicity of the surface bound magnetic beads should be addressed, micro-MACS has a great potential for high-throughput screening and commercial translation. Captured viable CTCs using magnetic nanoparticles (MNPs) in micro-MACS can be easily released

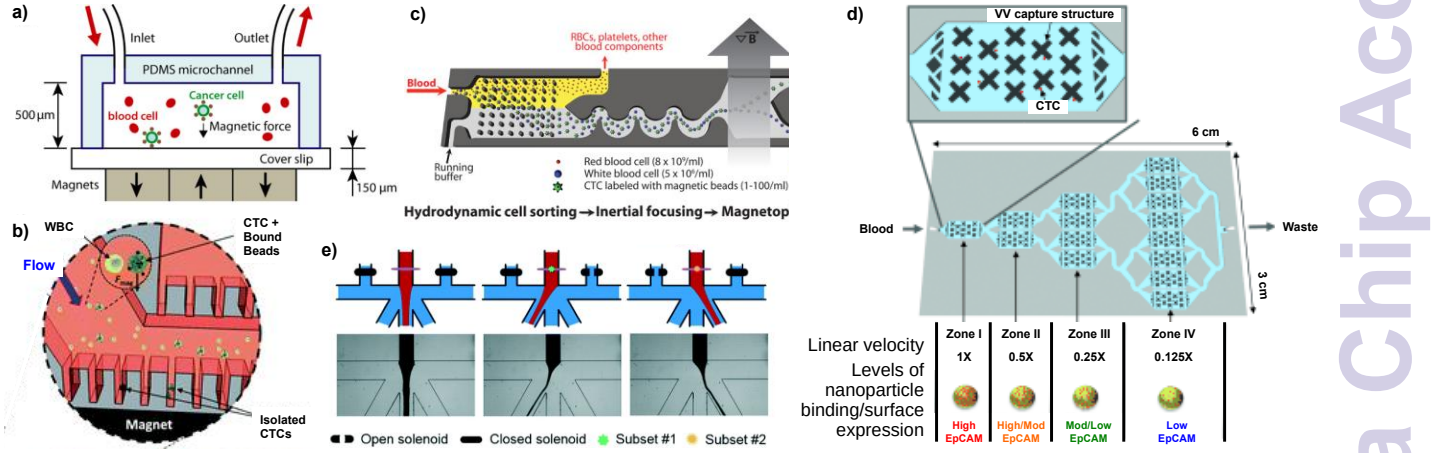


**Fig. 2**. Recent applications of micro-MACS and micro-FACS for CTC capture and identification. (a) A schematic illustration of CTC separation in the microchannel under a magnetic field after labelling with anti-EpCAM-functionalized magnetic nanoparticles. (Reproduced by permission of Royal Society of Chemistry) (b) The magnetic nanoparticle-bound CTCs were isolated in a unique microfluidic device containing an angled inlet channel and collection channels. The collection channels in the microchannel have arrays of dead-end side chambers (50 × 6 × 50 µm square with a gap of 100 µm) due to a permanent magnet beneath the lower row of side chambers. (Reproduced by permission of Royal Society of Chemistry) (c) The magnetic nanoparticle-bound CTCs were sorted out from blood cells in a series of debulking, inertial focusing, and magnetic separation steps in the CTC-iChip system. (Reproduced by permission of American Association for the Advancement of Science) (d) Depending on the EpCAM-expression level on CTCs, the anti-EpCAM-magnetic nanoparticle-labeled CTCs were sorted in a device with multiple velocity valley zones with different linear velocities: $EpCAM^{High}$ cells trapped in zone I and $EpCAM^{Low}$ cells trapped in zone IV. (Reproduced by permission of WILEY-VCH Verlag GmbH & Co. KGaA, Weinheim) (e) The separation mechanism of micro-FACS, dual-capture eDAR. After immunostaining blood samples, the active sorter in the microfluidic device was able to simultaneously separate the samples into 3 different channels: non-labeled to the center waste channel (left); green-labeled cells to the left isolation channel (middle); and red-labeled cells to the right isolation channel (right). (Reproduced by permission of Royal Society of Chemistry)

and recovered by removing a magnet. However, magnetic-activated sorting of cells from whole blood may change cell function or activity after binding with the paramagnetic beads.[41]

MNPs to magnetically capture and identify CTCs have been shown to efficiently lead to CTC isolation using micro-MACS. After conjugation with anti-EpCAM, $Fe_3O_4$ MNPs were added to cancer cell-spiked blood samples in a way identical to the procedure of the bench-top CellSearch™ system.[42] As an external force, a defined magnetic field gradient in the vicinity of arrayed magnets with alternating polarities, as illustrated in **Fig. 2a**, were applied to a typical PDMS microfluidic chip. This micro-MACS led to an effective capture of MNP-labeled cancer cells, resulting in 90% and 86% recovery rates of an $EpCAM^{low}$ colon cancer cell line, COLO205, and an $EpCAM^{high}$ breast cancer cell line, SKBR3 cells, respectively.[42] Compared to the CellSearch™ system, this micro-MACS required 25% fewer magnetic particles to achieve a comparable capture rate, while maintaining a fast screening speed (at an optimal blood flow rate of 10 mL $hr^{-1}$).[42]

Under a magnetic field, a microfluidic device with a main channel and multiple collection-channels lined in dead-end side chambers was demonstrated to isolate and trap magnetic beads-bound CTCs.[39] First, CTCs in blood were labeled with anti-EpCAM-coated magnetic microbeads (2.8 μm in diameter). Then magnetically labeled CTCs were isolated within the dead-end side chambers of the micro-MACS device with an angled inlet conduit (**Fig. 2b**). Design and dimensions of the microfluidic channels were optimized to maximize capture efficiency and to protect the isolated cells from shear stresses and stress-induced changes in cell physiology and behavior such as proliferation. This micro-MACS was able to isolate CTCs from mouse blood with high efficiency (~90%), specificity (0.4% blood cell capture), and viability (~90%). Additionally, the captured CTCs within its dead-end side chambers were expanded in culture after the removal of magnets from the device.

Magnetically driven collection of CTCs can be combined with cell sorting using hydrodynamic flow created in a microfluidic device. For instance, after immunolabeling of either CTCs or leukocytes using MNPs, inertial focusing in a microchannel induced alignment of CTCs and leukocytes following debulking that removed erythrocytes, platelets, and free MNPs (**Fig. 2c**). This alignment process allowed continuous, high-throughput separation of the nucleated cells.[40, 43] CTCs were then separated from leukocytes by either positive or negative selection using magnetophoresis.[40, 43] Another example shown in **Figure 2d** utilized the local velocity valleys (VVs) generated in a multizone microfluidic device to sort a cancer cell mixture into several subpopulations depending on the levels of EpCAM expression.[45] The multizone microfluidic device consisted of four different regions with different linear velocities: $EpCAM^{high}$ cells trapped in zone I (1X speed); $EpCAM^{medium}$ cells trapped in zone II – III (0.5X and 0.25X speed); and $EpCAM^{low}$ cells trapped in zone IV (0.125 X speed). The surface-marker-guided sorting and profiling of target cells in the multizone microfluidic device were successfully applied for *in vitro* cancer cell lines with varying surface expression as well as clinical blood samples from prostate cancer patients.[45]

**2.1.5. micro-FACS** FACS has been widely used to sort heterogeneous mixtures of cells into multiple populations of pure cell suspension based on fluorescent signals. FACS is automated, robust, and specific with outstanding sorting speeds (up to 50,000 cells per second). Similar to MACS relying on magnetic labels and magnets, FACS requires sequential steps of fluorescent labeling, hydrodynamic flow focusing, laser detection, and cell sorting.[31] However, because of the lack of detection sensitivity to separate rare cells, FACS is usually considered to be more suitable to sort out cells that represent a relatively major portion in the mixture.[12]

Recent development in nanotechnology and microfluidic technology enables the miniaturization of bench-top FACS systems. For example, to adapt FACS for CTC isolation, the Chiu group developed a process called "ensemble-decision aliquot ranking" (eDAR) and applied it to micro-FACS.[46, 47] Similar to FACS, the target cells were first labeled with fluorescence-tagged antibodies. However, instead of simultaneous cell analysis and sorting in conventional FACS, the eDAR process divided the sample into aliquots containing thousands of cells, and then detected fluorescent CTCs in each aliquot with pulsed lasers (**Fig. 2e**). The virtual aliquot volume in eDAR was optimized at 2 nL for system throughput (3 mL $h^{-1}$), which resulted in around 93% of capture efficiency for both MCF-7 and SKBR-3 cells at a low concentration of 5 cells $mL^{-1}$. In addition, by implementing multiple light sources and detectors as well as a variable direction high-speed active sorter, eDAR simultaneously and selectively performed multi-color sorting of two cell subsets. A heterogeneous mixture of rare cells from whole blood was labeled with two types of fluorescence-tagged antibodies against EpCAM and epidermal growth factor receptor (EGFR). The dual capture eDAR device with an active sorter demonstrated the simultaneous isolation of EpCAM+ and EGFR+ cancer cells with the improved recovery yields (~88%) at 50 μL $min^{-1}$.

Multiple functions can be successfully integrated in high-throughput, interdisciplinary microfluidic devices; however, this multifunctionalization often makes the design, fabrication, and operation of the devices complicated. The fabrication of complex devices would require technical expertise and long preparation time, and be challenging to scale up for volume production and large-scale clinical applications.[19] Those methods using hard-to-fabricate devices may have issues of inconsistency in quality control, analytical validation, and device fabrication for their clinical acceptance.[19, 48] Furthermore, these structured mirochannels would require a long time for full-field scanning to find the cells captured at vertically different locations.[49] In order to truly benefit from the miniaturization for CTC detection, other instruments in the detection process (e.g. a fluorescence detector with laser sources and optics) also need to be modified for wide-field imaging for low frequency CTC detection at high throughput without scarifying image resolution.[49]

The turnaround time of microfluidic devices also needs to be improved for high-throughput analysis of clinical samples. Due to the rarity of CTCs in blood, a fixed volume of 7.5 mL blood is typically processed for CTC capture as CellSearch® does. The volume capacity of a microchannel is typically less than 100 µL, which is too small to process 7.5 mL of blood in a reasonable time.[20] Even without considering the time to stain and scan the chip to find and count CTCs among a lot of hematological cells, it could take several hours to process the blood from a single patient.[20] It is a challenge for clinical laboratories to complete clinical scale samples for CTC detection as a routine assay at this sample processing speed.[19] Moreover, this long turnaround time, in addition to high shear stresses and potential clogging issue of blood clots or CTC clusters in microchannels, may adversely affect viability and function of captured CTC, making phenotyping and genotyping difficult.[20, 50]

### 2.2. Integration capability of microfluidic devices

Another important aspect of PDMS microfluidic devices is that they can be easily integrated with nanotechnologies to improve their performance, owing to several of the unique characteristics, such as: i) rapid fabrication by casting the PDMS polymer against photolithography-based molds;[51] ii) optical transparency and high elasticity;[52] iii) low magnetic susceptibility of PDMS polymers;[52] and iv) facile surface functionalization using silane chemicals. The characteristic rapid and inexpensive prototyping of PDMS microfluidic devices with high fidelity can reduce time and cost for a cycle of design, as well as fabricate and test several prototypes to optimize design parameters such as channel size and geometry. Elastomeric and optically transparent PDMS is an excellent material to be used under pressure since its surface can withstand high pressure under flow without deformation and be easily observed under a microscope, respectively. Thus PDMS microfluidic chamber with these characteristics enable to be integrated with nanostructured substrates functionalized for CTC capture. Low magnetic susceptibility could find use in systems for transport, positioning, separation, and sorting of magnetically labeled CTCs using magnetic forces, which can be combined with magnetic beads-based CTC detection. Hydrophilic silanol groups (Si-OH) can be easily derived on the hydrophobic surface of PDMS from its repeating unit of $–O-Si(CH_3)_2-$ via exposure to air and oxygen plasma oxidation.[51] The surface of PDMS or glass substrates could be functionalized with self-assembled monolayers of silane chemicals, which can be further chemically modified.[51] In addition, the functionalized PDMS devices are prone to wet with aqueous solutions and are less friendly to the adsorption of other hydrophobic species. The capability for surface functionalization on PDMS microfluidic devices is suitable to be developed as a multifunctional device via addition of polymers for controlled surface chemistries and additional functions (e.g. releasing capability of captured cells). For these reasons, PDMS microfluidic devices can easily adapt integrated analytical systems for CTC separation.

**2.2.1. Integration with nanostructured substrates** Nanostructured silicon substrates with highly dense arrays of uniform vertical silicon nanowires exhibit a high surface-to-volume ratio and the enhanced sensitivity for biomolecule detection in biosensors.[53, 54] The silicon nanowire arrays (SiNWAs) have unique structural features, excellent electronic, optical, thermoelectric, and mechanical properties, and biocompatibility with potential for various biomedical applications.[54] For example, compared with flat silicon substrates, SiNWAs with large surface areas were used as a platform for the enhanced capture of CTCs through incorporation into a PDMS microfluidic device.[55]

Anti-EpCAM-coated SiNWAs with a specific 3D nanostructure were integrated into a microfluidic system, named NanoVelcro chip, to increase the cell–substrate contact frequency and improve CTC-binding affinity.[56] After curing with aminosiloxane, the 3D surface on the SiNWAs and the integrated microfluidic devices were conjugated with streptavidin and biotinylated anti-EpCAM. This NanoVelcro system contained patterned SiNWAs coated with anti-EpCAM for high-affinity cell enrichment and a microfluidic device with a serpentine chaotic mixing channel capable of improving the CTC/substrate contact frequency (**Fig. 3a**). The synergistic effects led to high CTC-capture performance being observed for both spiked and clinical blood samples, which could potentially provide a convenient and cost-efficient alternative for sorting CTCs in clinic. After modifications with thermally responsive polymers, the CTC capture and release from NanoVelcro system were well controlled upon external temperature changes.[57] This thermally responsive NanoVelcro system demonstrated the effective capture of tumor cells from blood at 37°C and release of the captured cells with retained viability and functionality at 4°C, which will be further described in section 2.2.5 for integration of releasing capability.

**2.2.2. Combination with magnetic beads** Magnetic MNPs can form self-assembled structures in microfluidic devices under a magnetic field and be functionalized for CTC capture. Ephesia, a system of microfluidic channels with arrays of self-assembled biofunctionalized superparamagnetic beads was developed using a hexagonal array of magnetic ink patterned at the bottom of a PDMS microfluidic channel, after injecting anti-EpCAM-coated magnetic beads into the channel.[58] Upon exposure to the vertically applied external magnetic field, three-dimensional arrays of bead columns were formed and localized on top of the magnetic ink dots (**Fig. 3b**).[58] The integrated magnetic beads increased anti-EpCAM per surface area to efficiently bind to CTCs. The captured cells from patient samples in the Ephesia system were released for post-capture analysis of mutation detection by removing a magnet.[59] For example, heterozygous for E545K mutation on exon 9 of the PIK3CA gene were monitored on the released CTCs, which revealed its potential of this technology for post-capture genotyping.[59]

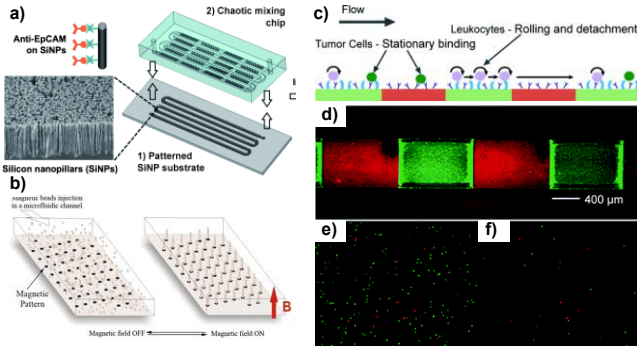


**Fig 3**. Application examples of microfluidic devices integrated with nanotechnology for CTC capture. (a) A PDMS microfluidic device with a microchannel was assembled with nanostructured silicon arrays, which was further functionalized with anti-EpCAM for CTC capture. The increased surface area through integration with nanostructured surface demonstrated the enhanced CTC sensitivity, compared to a flat chip. (Reproduced by permission of WILEY-VCH Verlag GmbH & Co. KGaA, Weinheim) (b) Anti-EpCAM-coated magnetic nanoparticles were injected and arrayed inside a microfluidic device under an external vertical magnetic field, which was used to functionalize the microfluidic device for CTC capture as well as to release the captured CTCs after removing the magnet. (Reproduced by permission of National Academy of Sciences) (c-f) A micropatterned microfluidic device integrated with nanomaterials and biomimetic proteins, such as dendrimers and E-selectin, respectively, significantly increases the CTC capture efficiency and purity under flow conditions. An alternating pattern of the immobilized anti-EpCAM-dendrimer (red, d) and E-selectin (green, d) on a PDMS channel surface showed stationary tumor cell binding (red dots, e) across the entire capture surface, while leukocytes rolling (green dots, e) on E-selectin patterns. After rinsing with a leukocyte elution buffer, the enrichment of red-labeled tumor cells on the surface was clearly shown in (f). (Reproduced by permission of American Chemical Society)

**2.2.3. Addition of polymers for controlled surface chemistries** Recent advances in polymeric nanomaterials have enabled the design of biomedical devices with significantly improved performance. For example, multivalent binding that occurs in a variety of physiological processes has been exploited to significantly increase the sensitivity and selectivity of detection assays.[60] We have used poly(amidoamine) (PAMAM) dendrimers that allow precisely control the multivalent binding effect with their characteristic properties obtained from their well-defined chemical structure, a high density of peripheral functional groups, and easy deformability.[61, 62] The binding strength between CTCs and a capture surface can be enhanced through dendrimer-mediated multivalent binding effect, which can significantly improve the sensitivity and selectivity of the surfaces for CTC detection.[62, 63] Compared to that on the linear polymer-coated surface, the surfaces functionalized with the anti-EpCAM-dendrimer conjugates exhibited dramatically enhanced cell adhesion and binding stability of three breast cancer cell lines (MDA-MB-361, MCF-7, and MDA-MB-231).[62] In addition, immobilization of E-selectin induced cell rolling and has been shown to enhance the surface capture of tumor cells (up to 10 fold compared to the same surface without dendrimers).[63-65] We have also applied the significant enhancement of the dendrimer-coated surfaces to various antibodies and have shown the effectiveness of the device in capturing tumor cells from clinically relevant blood samples as well.[63]

The biomimetic combination of the anti-EpCAM-dendrimer conjugates and E-selectin has been introduced into microfluidic channels. The *in situ* patterning of the two proteins onto the inside of a permanently bonded PDMS microfluidic device has been shown to improve immunoaffinity-based tumor cell capture.[66] Micropatterned photopolymerized poly(acrylic acid) (PAA) with carboxyl termini on the PDMS microchannels were used for E-selectin attachment using 1-ethyl-3-(3-dimethylaminopropyl) carbodiimide (EDC)/N-hydroxysulfosuccinimide (NHS) coupling. Then, the self-assembled monolayers of (3-mercaptopropyl)trimethoxysilane with sulfhydryl groups backfilled between PAA patterns on the PDMS microchannels were used for surface immobilization of the anti-EpCAM-dendrimer conjugates using an N-maleimidobutyryl-oxysuccinimide ester (GMBS) cross-linker (**Fig. 3c**). By patterning the two adhesive proteins in an alternating way, the specificity and sensitivity for tumor cell capture were significantly increased under flow. This *in situ* pattern of alternating biomimetic proteins reduced leukocyte capture by up to 82%, while maintaining a high tumor cell capture efficiency up to 1.9 times higher than the tumor cell capture efficiency of a surface with anti-EpCAM only. Moreover, this patterning technique requires no mask alignment and can be used to spatially control the immobilization of multiple proteins inside a sealed microchannel.

**2.2.4. Incorporation of releasing capability** CTCs captured from patient blood provide opportunities to perform post-capture analysis to identify signaling pathways and investigate molecular profiling of the individual CTCs. A number of approaches to efficiently release the captured CTCs have been explored to facilitate subsequent cell culture and single-cell analyses.[67, 68] A promising approach is to use stimuli-responsive polymers for CTC capture and release. The stimuli-responsive polymers have been used to release the captured CTCs upon exposure to various stimuli, such as light, temperature, pH, and physical stress. Proteolytic enzymes and/or stimuli-responsive polymers have been commonly used to engineer the CTC capture surface to release the cells as a result of surface degradation or in response to the external stimuli.

Alginate hydrogels have been incorporated onto the surface to increase CTC capture efficiency by altering the surface topography and efficiently release the isolated CTCs from the surface upon simple stimulation. Alginate in solution containing $CaCl_2$ was injected into the 1st generation CTC-chip for *in situ* hydrogel formation on the chip surface, which was further functionalized with a mixture of PEG, EDC, sulfo-NHS and anti-CD34. This ionically crosslinked hydrogel was used to capture and release CD34-expressing endothelial progenitor cells in heparin-treated blood specimens without the need for enzymatic digestion,[67] with the principle of calcium chelation driving the substrate degradation. When the alginate hydrogel on the chip surface were covalently crosslinked using a photoinitiator irgacure 2959 and functionalized with anti-EpCAM, EpCAM-expressing CTCs were captured and released via a treatment with alginate lyase (**Fig. 4a**).[69] This calcium-sensitive approach is limited by the fact that the chelating agents, such as ethylenediaminetetraacetic acid (EDTA), cannot be used as blood anticoagulants. The use of enzymes (alginate lyase and DNase) has also resulted in poor efficiency (<10%) in release and limited viability of the cells.[57]

Self-assembled DNA nanostructures were incorporated onto the avidin-coated, herringbone microfluidic device via rolling circle amplification at 37°C using a biotinylated primer-circular template complex, nucleotide triphosphate containing deoxyribose (dNTP), and DNA polymerase (**Fig. 4b**).[70] Multiple long aptamers in the matrix of the DNA nanostructures on the chip had highly specific binding affinity with lymphoblast CCRF-CEM cells over monovalent aptamers and anti-EpCAM.[70] The degradation of DNA matrix under exposure to DNase/endonucleases induced the release of captured cells from the chip.[70]

As discussed earlier in section 2.2.2, the thermally responsive NanoVelcro system demonstrated the effective capture and release of tumor cells from blood upon external temperature changes. In this study, thermally responsive poly(*N*-isopropylacrylamide) (PNIPAAm) polymers were grafted onto a silicon nanowire array (SiNWAs)-based CTC detection platform.[57] The amino groups on the PNIPAAm-grafted NanoVelcro were then conjugated with biotin-NHS and streptavidin for further functionalization with biotinylated anti-EpCAM. As shown in **Fig. 4c,** this thermally responsive platform demonstrated the effective capture of tumor cells in the presence of human blood cells at 37°C and release of the captured cells with retained viability and functionality at 4°C. The PNIPAAm-grafted NanoVelcro exhibited reversible cellular attachment and detachment in response to temperature due to the transition of the chain conformation between the hydrophobic collapsed state and the hydrophilic extended state. At 37°C, biotins were present on the surfaces, leading to the binding of biotinylated anti-EpCAM through a streptavidin as a bridge and thus facilitating the capture of cancer cells with high efficiency. As the temperature decreased to 4°C, the PNIPAAm chains became hydrophilic and extended to encapsulate the anti-EpCAM, which stimulated the release of captured cells.

A thermally responsive gelatin-based nanostructured coating by a layer-by-layer (LbL) deposition of biotinylated gelatin and streptavidin was also developed for temperature-responsive release (for bulk-population recovery) of captured CTCs (**Fig. 4d**).[68] Raising the device temperature to 37°C degraded the nanocoating from the whole surface within minutes for a bulk-population release of CTCs. In addition, local regions of the gelatin nanocoating were sensitive to mechanical stresses from a frequency-controlled microtip, which was used for mechanosensitive single cell release of CTCs (**Fig. 4d**).[68] This dual release strategy from the gelatin-coated chip has successfully driven the characterization of the PIK3CA and EGFR oncogene mutations in the released CTCs.

Although promising, it should be noted that these stimuli-responsive nanomaterials may face challenges to be clinically implemented due to the requirement to run the samples at

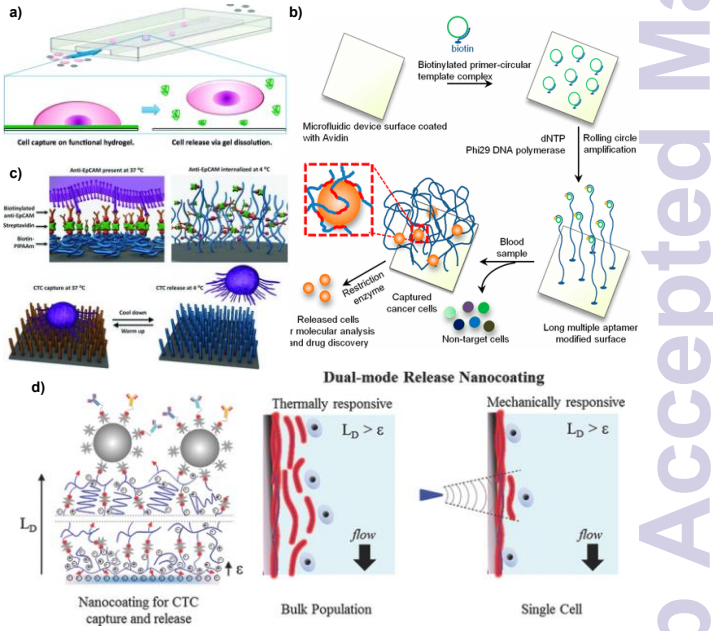


**Fig. 4**. Releasing capability-integrated microfluidic devices for CTC capture and release. (a) An alginate gel-coated microfluidic device was able to capture CTCs after anti-EpCAM functionalization, as well as to release the captured CTCs via gel dissolution after brief exposure to the bacterial enzyme, alginate lyase. (Reproduced by permission of American Chemical Society) (b) A microfluidic device incorporated with long multivalent DNA aptamer isolated CTCs from whole blood which were released after DNase treatment to cleave DNA aptamers on the surface. (Reproduced by permission of National Academy of Sciences) (c) A schematic illustration of a microfluidic device integrated with a nanostructured silicon surface and thermally responsive polymers, such as PNIPAAm. The captured CTCs on the nanomaterial-based device at 37°C were released after lowering temperature to 4°C. (Reproduced by permission of WILEY-VCH Verlag GmbH & Co. KGaA, Weinheim) (d) The multiple layer-by-layer deposition of biotinylated gelatin and streptavidin on the surface of a microfluidic device was able to isolate and release CTCs from the nanocoating in two different mechanisms: bulk cell release via temperature changes (left); and the single cell/selective release after applying localized shear stress via inducing vibration of the microtip (right). (Reproduced by permission of WILEY-VCH Verlag GmbH & Co. KGaA, Weinheim)

certain temperature (for thermally responsive nanomaterials) and conditions (DNase/endonuclease-free conditions for DNA/aptamer-based materials). Additionally, the exposure of individual cells to a certain stimulus (e.g. enzyme, light, chemical, temperature, or mechanical stress) during the release process may affect the cell viability. In addition, the nanomaterial-integrated microfluidic device may have some potential issues regarding stability and quality control due to intrinsic heterogeneous and often unstable characteristics of nanomaterials.

### 2.3. *In situ* or sequential analysis of isolated CTCs

The genetic information of enumerated CTCs at the level of a single cell will significantly contribute to a better understanding of CTC population through complete characterization and functional analysis. The single-cell genetics of low-frequency CTCs may provide the means to link genetic data to new insights of the complex mechanisms of drug resistance, ultimately leading to the development of personalized cancer treatments. Research incorporating microfluidics and single-cell genetic analysis, including cell capture and enrichment, cell compartmentalization, and detection, can be used to create simple and more informative tools for CTC studies.[71] Microfluidic technologies are attractive for single-cell manipulation due to precise handling to isolate rare CTCs and low risk of contamination from the environment and components within the sample.[12] Microfluidic single-cell techniques can also allow for high-throughput and detailed genetic analyses that increase accuracy with reduced cost, compared to bulk techniques.[12] Additionally, microfluidic technologies provide an additional option to *in situ* culture of live and intact CTCs for down-stream analysis due to PDMS's unique properties of optical transparency, flexibility, high permeability to gases of water, oxygen, and chemicals.[52, 72] Incorporating these microfluidic platforms into research and clinical laboratory workflows can fill an unmet need in biology, delivering highly accurate, informative data necessary to develop new therapies and monitor patient outcomes.

**2.3.1. *in situ* analysis while capturing** Enrichment must be used in line with the separation system to reduce the contamination possibilities and the liquid volume for rapid detection and analysis. To clean up unnecessary hematological cells, a variety of detection strategies, such as layers with 8 μm pores for size-based filtration[73] and magnetic or physical traps,[74] were incorporated to microfluidic systems for CTC detection and *in situ* analysis. Optically transparent PDMS microfluidic devices allow to identify the captured and washed CTCs through immunofluorescence staining against cytokeratin, CD45, and DAPI on chip, and perform the subsequent *in situ* analysis for the single-cell genetic profiling of the CTCs.

Fluorescence *in situ* hybridization (FISH) has been frequently used for *in situ* analysis and successfully evaluated the amplification status of cancer-related genes in microfluidic devices. The 2nd generation CTC chip with a herringbone pattern[75] was used to successfully isolate pancreatic CTCs from mouse and human blood and to investigate the molecular characterization of signaling pathways associated with proliferation and anoikis (a form of programmed cell death that is induced by anchorage-dependent cells detaching from the surrounding extracellular matrix)(**Fig. 5a**).[76] Expression of WNT in pancreatic cancer cells is known to suppress anoikis, enhance anchorage-independent sphere formation, and increase metastatic propensity *in vivo*.[76] The results of single-molecule RNA sequencing showed the amplification of WNT signaling genes of captured CTCs in 5 out of 11 cases of pancreatic cancer patients, demonstrating that the WNT signaling pathways may contribute to pancreatic cancer metastasis. The treatment of WNT inhibitors, TAK1 inhibitor and shTak1, on tumor cells clearly showed the increased anchorage-independent tumor sphere formation. Thus, the effectiveness of WNT inhibition in suppressing this effect could potentially identify a novel drug target for metastasis suppression to prevent the distal spread of cancer.[75]

**2.3.2. Sequential analysis** Through concentrating rare cells in localized regions with microfluidic systems, mechanical traps are some of the most commonly used methods that anchor particles and cells to a physical structure and enable multistep perfusion of reagents to perform cell assays on-chip. After capturing, it is important to release particles and cells on demand for further downstream analysis.[74, 77] Having discussed regarding stimuli-responsive polymers for the release of the captured cells from these microfluidic devices in section 2.2.4, this section will focus on other approaches to collect the CTCs for downstream, sequential analyses.

Swennenhuis, J.F. et al developed a microfluidic device with microwells to capture and recover CTCs.[74] The captured and identified CTCs on the multiwell microfluidic device were collected by punching the bottom of the device. The self-seeding chip contained 6,400 microwells (a diameter of 70 μm and depth of 360 μm) to trap a single cell per well (**Fig. 5b**). A 5 μm pore-size filter was placed in the center of the microwell to allow for media or non-target cells to pass through, removing unnecessary background signals. After fast and efficient distribution of single cells in individual microwells by applying a negative pressure of 10 mbar under the slide using an air pump, manometer, and a pressure regulator, the cells of interest in the microwells were recovered into a 96 PCR well plate by punching the 1 μm thick bottom. The recovered cells were used for the DNA amplification and Sanger sequencing.[74] The signatures of ROBO2 and PTEN genes in the recovered PC-3 cells were identified, which was used to determine the capture specificity.[74] Instead of punching the wall of microfluidic device, other approaches, including the use of a suction needle for single cell retrieval, could be also combined with microfluidic devices to recover the captured CTCs for sequential analysis.[78]

## Conclusions

Accurate CTC detection has great potential to provide valuable clinical insight into the progress of metastatic cancers and to monitor responses of patients during cancer therapy. As summarized in this review, recent advances in microfluidics, through miniaturization of bench-top analytical instruments, integration with nanotechnology, and capability of *in situ* analysis of captured CTCs, have provided various designs and promising implementation of highly reliable CTC-capture platforms with excellent yield and selectivity. However, microfluidic devices, especially PDMS-based, have potential difficulties to be translated for clinical impact. For clinical translation, next generation of CTC microfluidic devices is expected to meet the following standards: i) enhanced detection sensitivity and specificity than the current CTC devices; ii) shorter total analytical time for CTC detection, capture, and identification; iii) enhanced capability for *in situ* or sequential analysis after capturing; iv) simplification of operating procedures for high-throughput; and v) minimal batch-to-batch variations. Beyond simple enumeration, *in situ* analysis of the captured CTCs on microfluidic devices will lead to novel insight into cancer progression and metastasis, and genetic/phenotypic changes of cancer cells. We expect that such CTC microfluidic devices will be implemented for the routine use in point-of-care testing and ultimately play a key role in achieving personalized therapeutics for cancer patients.

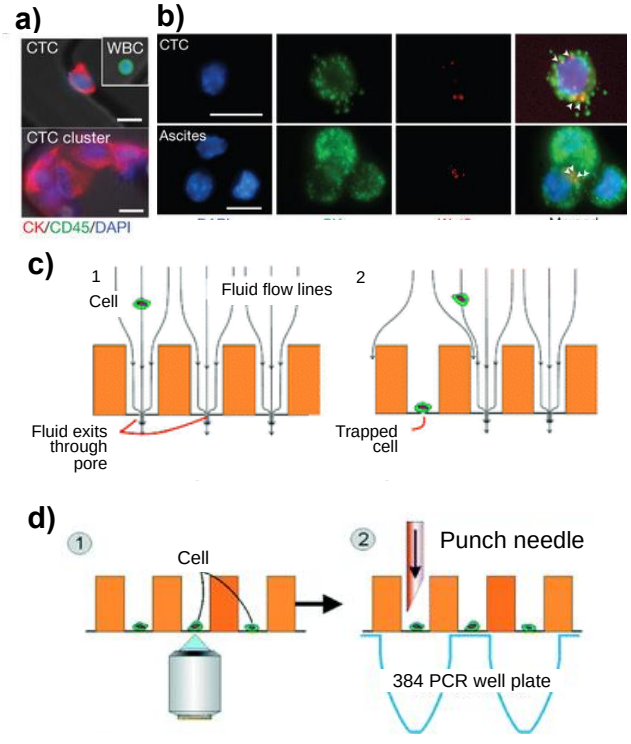


**Fig. 5**. Microfluidic device applications for *in situ* or sequential analysis of the captured CTCs. (a-b) Immunofluorescence staining (a) and RNA-in situ hybridization (RNA-ISH), b) of mouse pancreatic CTCs on the microfluidic device. (a) Green-labelled leukocytes and red-labelled CTC clusters were identified *in situ* (DAPI, blue; cytokeratin (CK), red; CD45, green). (b) RNA-ISH of CTCs showed the co-expression of CK8+18 (green) and *Wnt2* (red) transcripts. (Reproduced by permission of Nature Publishing Group) (c-d) Direct collection of single CTCs per microwells for sequential analysis. (c) While leukocytes or other blood components were passing through a small hole on the bottom, the CTCs were trapped in the microwell with a diameter of 70 μm and depth of 360 μm. After identifying the trapped cells as CTCs, single cell per microwell were acquired to 384 well plate via punching the silicon bottom using a punch needle. (Reproduced by permission of Royal Society of Chemistry)

## Acknowledgements

This work was supported by National Cancer Institute (NCI), National Institutes of Health (NIH) under grant # R01-CA182528, National Science Foundation (NSF) under grant # DMR-1409161, and the Technological Innovation R&D Program (grant # S2083505) funded by the Small and Medium Business Administration of Korea.

## References

1. S. Riethdorf, H. Fritsche, V. Muller, T. Rau, C. Schindlbeck, B. Rack, W. Janni, C. Coith, K. Beck, F. Janicke, S. Jackson, T. Gornet, M. Cristofanilli and K. Pantel, *Clin. Cancer Res.*, 2007, **13**, 920-928.
2. M. Cristofanilli, G. T. Budd, M. J. Ellis, A. Stopeck, J. Matera, M. C. Miller, J. M. Reuben, G. V. Doyle, W. J. Allard, L. W. Terstappen and D. F. Hayes, *N. Engl. J. Med.*, 2004, **351**, 781-791.
3. A. van de Stolpe, K. Pantel, S. Sleijfer, L. W. Terstappen and J. M. den Toonder, *Cancer Res.*, 2011, **71**, 5955-5960.
4. S. Paget, *Cancer Metastasis Rev.*, 1989, **8**, 98-101.
5. J. H. Myung, K. A. Gajjar, Y. E. Han and S. P. Hong, *Polym. Chem.-UK*, 2012, **3**, 2336-2341.
6. J. H. Myung, K. A. Tam, S. Park, A. Cha and S. Hong, *WIREs Nanomed. Nanobiotechnol.* 2015, DOI: 10.1002/wnan.1360.
7. N. Saucedo-Zeni, S. Mewes, R. Niestroj, L. Gasiorowski, D. Murawa, P. Nowaczyk, T. Tomasi, E. Weber, G. Dworacki, N. G. Morgenthaler, H. Jansen, C. Propping, K. Sterzynska, W. Dyszkiewicz, M. Zabel, M. Kiechle, U. Reuning, M. Schmitt and K. Lucke, *Int. J. Oncol.*, 2012, **41**, 1241-1250.
8. W. J. Allard, J. Matera, M. C. Miller, M. Repollet, M. C. Connelly, C. Rao, A. G. Tibbe, J. W. Uhr and L. W. Terstappen, *Clin. Cancer Res.*, 2004, **10**, 6897-6904.
9. A. J. Armstrong, M. S. Marengo, S. Oltean, G. Kemeny, R. L. Bitting, J. D. Turnbull, C. I. Herold, P. K. Marcom, D. J. George and M. A. Garcia-Blanco, *Mol. Cancer Res.*, 2011, **9**, 997-1007.
10. S. K. Arya, B. Lim and A. R. Rahman, *Lab Chip*, 2013, **13**, 1995-2027.
11. I. Cima, C. Wen Yee, F. S. Iliescu, W. M. Phyo, K. H. Lim, C. Iliescu and M. H. Tan, *Biomicrofluidics*, 2013, **7**, 11810.
12. Y. Dong, A. M. Skelley, K. D. Merdek, K. M. Sprott, C. Jiang, W. E. Pierceall, J. Lin, M. Stocum, W. P. Carney and D. A. Smirnov, *J. Mol. Diagn.*, 2013, **15**, 149-157.
13. P. R. Gascoyne and S. Shim, *Cancers*, 2014, **6**, 545-579.
14. V. Gupta, I. Jafferji, M. Garza, V. O. Melnikova, D. K. Hasegawa, R. Pethig and D. W. Davis, *Biomicrofluidics*, 2012, **6**, 24133.
15. C. Jin, S. M. McFaul, S. P. Duffy, X. Deng, P. Tavassoli, P. C. Black and H. Ma, *Lab Chip*, 2014, **14**, 32-44.
16. L. Hajba and A. Guttman, *Trends Anal. Chem.*, 2014, **59**, 9-16.

17. P. N. Nge, C. I. Rogers and A. T. Woolley, *Chem. Rev.*, 2013, **113**, 2550-2583.
18. J. El-Ali, P. K. Sorger and K. F. Jensen, *Nature*, 2006, **442**, 403-411.
19. C. D. Chin, V. Linder and S. K. Sia, *Lab Chip*, 2012, **12**, 2118-2134.
20. B. Hong and Y. L. Zu, *Theranostics*, 2013, **3**, 377-394.
21. P. Chen, Y. Y. Huang, K. Hoshino and X. Zhang, *Lab Chip*, 2014, **14**, 446-458.
22. S. Zheng, H. Lin, J. Q. Liu, M. Balic, R. Datar, R. J. Cote and Y. C. Tai, *J. Chromatogr. A*, 2007, **1162**, 154-161.
23. G. Attard, M. Crespo, A. C. Lim, L. Pope, A. Zivi and J. S. de Bono, *Clin. Cancer Res.*, 2011, **17**, 3048-3049; author reply 3050.
24. L. S. Lim, M. Hu, M. C. Huang, W. C. Cheong, A. T. Gan, X. L. Looi, S. M. Leong, E. S. Koay and M. H. Li, *Lab Chip*, 2012, **12**, 4388-4396.
25. A. Yusa, M. Toneri, T. Masuda, S. Ito, S. Yamamoto, M. Okochi, N. Kondo, H. Iwata, Y. Yatabe, Y. Ichinosawa, S. Kinuta, E. Kondo, H. Honda, F. Arai and H. Nakanishi, *Plos One*, 2014, **9**.
26. D. L. Adams, P. X. Zhu, O. V. Makarova, S. S. Martin, M. Charpentier, S. Chumsri, S. H. Li, P. Amstutz and C. M. Tang, *RSC Adv.*, 2014, **4**, 4334-4342.
27. J. H. Myung, M. Roengvoraphoj, K. A. Tam, T. Ma, V. A. Memoli, E. Dmitrovsky, S. J. Freemantle and S. Hong, *Anal. Chem.*, 2015, DOI: 10.1021/acs.analchem.5b02766.
28. D. Marrinucci, K. Bethel, R. H. Bruce, D. N. Curry, B. Hsieh, M. Humphrey, R. T. Krivacic, J. Kroener, L. Kroener, A. Ladanyi, N. H. Lazarus, J. Nieva and P. Kuhn, *Hum. Pathol.*, 2007, **38**, 514-519.
29. B. Molnar, A. Ladanyi, L. Tanko, L. Sreter and Z. Tulassay, *Clin. Cancer Res.*, 2001, **7**, 4080-4085.
30. N. Aceto, A. Bardia, D. T. Miyamoto, M. C. Donaldson, B. S. Wittner, J. A. Spencer, M. Yu, A. Pely, A. Engstrom, H. Zhu, B. W. Brannigan, R. Kapur, S. L. Stott, T. Shioda, S. Ramaswamy, D. T. Ting, C. P. Lin, M. Toner, D. A. Haber and S. Maheswaran, *Cell*, 2014, **158**, 1110-1122.
31. A. F. Sarioglu, N. Aceto, N. Kojic, M. C. Donaldson, M. Zeinali, B. Hamza, A. Engstrom, H. Zhu, T. K. Sundaresan, D. T. Miyamoto, X. Luo, A. Bardia, B. S. Wittner, S. Ramaswamy, T. Shioda, D. T. Ting, S. L. Stott, R. Kapur, S. Maheswaran, D. A. Haber and M. Toner, *Nat. Methods*, 2015, **12**, 685-691.
32. A. J. Mach, O. B. Adeyiga and D. Di Carlo, *Lab Chip*, 2013, **13**, 1011-1026.
33. A. J. Mach, J. H. Kim, A. Arshi, S. C. Hur and D. Di Carlo, *Lab Chip*, 2011, **11**, 2827-2834.
34. J. Che, A. J. Mach, D. E. Go, I. Talati, Y. Ying, J. Rao, R. P. Kulkarni and D. Di Carlo, *Plos One*, 2013, **8**, e78194.
35. A. M. Dupuy, S. Lehmann and J. P. Cristol, *Clin. Chem. Lab. Med.*, 2005, **43**, 1291-1302.
36. F. Olasagasti and J. C. Ruiz de Gordoa, *Transl. Res.*, 2012, **160**, 332-345.
37. S. Nagrath, L. V. Sequist, S. Maheswaran, D. W. Bell, D. Irimia, L. Ulkus, M. R. Smith, E. L. Kwak, S. Digumarthy, A. Muzikansky, P. Ryan, U. J. Balis, R. G. Tompkins, D. A. Haber and M. Toner, *Nature*, 2007, **450**, 1235-1239.
38. S. L. Stott, C. H. Hsu, D. I. Tsukrov, M. Yu, D. T. Miyamoto, B. A. Waltman, S. M. Rothenberg, A. M. Shah, M. E. Smas, G. K. Korir, F. P. Floyd, Jr., A. J. Gilman, J. B. Lord, D. Winokur, S. Springer, D. Irimia, S. Nagrath, L. V. Sequist, R. J. Lee, K. J. Isselbacher, S. Maheswaran, D. A. Haber and M. Toner, *Proc. Natl. Acad. Sci. U.S.A.*, 2010, **107**, 18392-18397.
39. J. H. Kang, S. Krause, H. Tobin, A. Mammoto, M. Kanapathipillai and D. E. Ingber, *Lab Chip*, 2012, **12**, 2175-2181.
40. E. Ozkumur, A. M. Shah, J. C. Ciciliano, B. L. Emmink, D. T. Miyamoto, E. Brachtel, M. Yu, P. I. Chen, B. Morgan, J. Trautwein, A. Kimura, S. Sengupta, S. L. Stott, N. M. Karabacak, T. A. Barber, J. R. Walsh, K. Smith, P. S. Spuhler, J. P. Sullivan, R. J. Lee, D. T. Ting, X. Luo, A. T. Shaw, A. Bardia, L. V. Sequist, D. N. Louis, S. Maheswaran, R. Kapur, D. A. Haber and M. Toner, *Sci. Transl. Med.*, 2013, **5**, 179ra147.
41. J. M. Oatley, M. J. Oatley, M. R. Avarbock, J. W. Tobias and R. L. Brinster, *Development*, 2009, **136**, 1191-1199.
42. K. Hoshino, Y. Y. Huang, N. Lane, M. Huebschman, J. W. Uhr, E. P. Frenkel and X. Zhang, *Lab Chip*, 2011, **11**, 3449-3457.
43. N. M. Karabacak, P. S. Spuhler, F. Fachin, E. J. Lim, V. Pai, E. Ozkumur, J. M. Martel, N. Kojic, K. Smith, P. I. Chen, J. Yang, H. Hwang, B. Morgan, J. Trautwein, T. A. Barber, S. L. Stott, S. Maheswaran, R. Kapur, D. A. Haber and M. Toner, *Nat. Protoc.*, 2014, **9**, 694-710.
44. J. H. Shin, M. G. Lee, S. Choi and J.-K. Park, *RSC Adv.*, 2014, **4**, 39140-39144.
45. R. M. Mohamadi, J. D. Besant, A. Mepham, B. Green, L. Mahmoudian, T. Gibbs, I. Ivanov, A. Malvea, J. Stojcic, A. Allan, L. E. Lowes, E. H. Sargent, R. K. Nam and S. O. Kelley, *Angew. Chem. Int. Ed. Engl.*, 2015, **54**, 139-143.
46. P. G. Schiro, M. Zhao, J. S. Kuo, K. M. Koehler, D. E. Sabath and D. T. Chiu, *Angew. Chem. Int. Ed. Engl.*, 2012, **51**, 4618-4622.
47. M. Zhao, B. Wei, W. C. Nelson, P. G. Schiro and D. T. Chiu, *Lab Chip*, 2015, DOI: 10.1039/C5LC00384A.
48. H. Becker, *Lab Chip*, 2010, **10**, 271-273.
49. J. Balsam, H. A. Bruck and A. Rasooly, *Analyst*, 2014, **139**, 4322-4329.
50. K. A. Hyun and H. I. Jung, *Lab Chip*, 2014, **14**, 45-56.
51. J. C. McDonald, D. C. Duffy, J. R. Anderson, D. T. Chiu, H. Wu, O. J. Schueller and G. M. Whitesides, *Electrophoresis*, 2000, **21**, 27-40.
52. P. C. H. Li, *Microfluidic lab-on-a-chip for chemical and biological analysis and discovery*, Taylor & Francis/CRC Press, Boca Raton, 2006.
53. Q. Yu, H. Liu and H. Chen, *J Mater Chem B*, 2014, **2**, 7849-7860.
54. L. Wang, W. Asghar, U. Demirci and Y. Wan, *Nano Today*, 2013, **8**, 347-387.
55. S. Wang, H. Wang, J. Jiao, K. J. Chen, G. E. Owens, K. Kamei, J. Sun, D. J. Sherman, C. P. Behrenbruch, H. Wu and H. R. Tseng, *Angew. Chem. Int. Ed. Engl.*, 2009, **48**, 8970-8973.
56. S. Wang, K. Liu, J. Liu, Z. T. Yu, X. Xu, L. Zhao, T. Lee, E. K. Lee, J. Reiss, Y. K. Lee, L. W. Chung, J. Huang, M. Rettig, D. Seligson, K. N. Duraiswamy, C. K. Shen and H. R. Tseng, *Angew. Chem. Int. Ed. Engl.*, 2011, **50**, 3084-3088.
57. S. Hou, H. C. Zhao, L. B. Zhao, Q. L. Shen, K. S. Wei, D. Y. Suh, A. Nakao, M. A. Garcia, M. Song, T. Lee, B. Xiong, S. C. Luo, H. R. Tseng and H. H. Yu, *Adv. Mater.*, 2013, **25**, 1547-1551.
58. A. E. Saliba, L. Saias, E. Psychari, N. Minc, D. Simon, F. C. Bidard, C. Mathiot, J. Y. Pierga, V. Fraisier, J. Salamero, V. Saada, F. Farace, P. Vielh, L. Malaquin and J. L. Viovy, *Proc. Natl. Acad. Sci. U.S.A.*, 2010, **107**, 14524-14529.
59. J. Autebert, B. Coudert, J. Champ, L. Saias, E. T. Guneri, R. Lebofsky, F.-C. Bidard, J.-Y. Pierga, F. Farace, S. Descroix, L. Malaquin and J.-L. Viovy, *Lab Chip*, 2015, **15**, 2090-2101.
60. M. Mammen, S. K. Choi and G. M. Whitesides, *Angew. Chem. Int. Ed. Engl.*, 1998, **37**, 2755-2794.
61. S. Hong, P. R. Leroueil, I. J. Majoros, B. G. Orr, J. R. Baker, Jr. and M. M. Banaszak Holl, *Chem. Biol.*, 2007, **14**, 107-115.
62. J. H. Myung, K. A. Gajjar, J. Saric, D. T. Eddington and S. Hong, *Angew. Chem. Int. Ed. Engl.*, 2011, **50**, 11769-11772.

63. J. H. Myung, K. A. Gajjar, J. H. Chen, R. E. Molokie and S. Hong, *Anal. Chem.*, 2014, **86**, 6088-6094.
64. J. H. Myung, C. A. Launiere, D. T. Eddington and S. Hong, *Langmuir*, 2010, **26**, 8589-8596.
65. J. H. Myung, K. A. Gajjar, R. M. Pearson, C. A. Launiere, D. T. Eddington and S. Hong, *Anal. Chem.*, 2011, **83**, 1078-1083.
66. C. Launiere, M. Gaskill, G. Czaplewski, J. H. Myung, S. Hong and D. T. Eddington, *Anal. Chem.*, 2012, **84**, 4022-4028.
67. A. Hatch, G. Hansmann and S. K. Murthy, *Langmuir*, 2011, **27**, 4257-4264.
68. E. Reategui, N. Aceto, E. J. Lim, J. P. Sullivan, A. E. Jensen, M. Zeinali, J. M. Martel, A. J. Aranyosi, W. Li, S. Castleberry, A. Bardia, L. V. Sequist, D. A. Haber, S. Maheswaran, P. T. Hammond, M. Toner and S. L. Stott, *Adv. Mater.*, 2015, **27**, 1593-1599.
69. A. M. Shah, M. Yu, Z. Nakamura, J. Ciciliano, M. Ulman, K. Kotz, S. L. Stott, S. Maheswaran, D. A. Haber and M. Toner, *Anal. Chem.*, 2012, DOI: 10.1021/ac300190j.
70. W. A. Zhao, C. H. Cui, S. Bose, D. G. Guo, C. Shen, W. P. Wong, K. Halvorsen, O. C. Farokhzad, G. S. L. Teo, J. A. Phillips, D. M. Dorfman, R. Karnik and J. M. Karp, *Proc. Natl. Acad. Sci. U.S.A.*, 2012, **109**, 19626-19631.
71. A. M. Thompson, A. L. Paguirigan, J. E. Kreutz, J. P. Radich and D. T. Chiu, *Lab Chip*, 2014, **14**, 3135-3142.
72. S. Halldorsson, E. Lucumi, R. Gomez-Sjoberg and R. M. T. Fleming, *Biosens. Bioelectron.*, 2015, **63**, 218-231.
73. C.-L. Chang, W. Huang, S. I. Jalal, B.-D. Chan, A. Mahmood, S. Shahda, B. H. O'Neil, D. E. Matei and C. A. Savran, *Lab Chip*, 2015, **15**, 1677-1688.
74. J. F. Swennenhuis, A. G. J. Tibbe, M. Stevens, M. R. Katika, J. van Dalum, H. Duy Tong, C. J. M. van Rijn and L. W. M. M. Terstappen, *Lab Chip*, 2015, **15**, 3039-3046.
75. M. Yu, D. T. Ting, S. L. Stott, B. S. Wittner, F. Ozsolak, S. Paul, J. C. Ciciliano, M. E. Smas, D. Winokur, A. J. Gilman, M. J. Ulman, K. Xega, G. Contino, B. Alagesan, B. W. Brannigan, P. M. Milos, D. P. Ryan, L. V. Sequist, N. Bardeesy, S. Ramaswamy, M. Toner, S. Maheswaran and D. A. Haber, *Nature*, 2012, **487**, 510-513.
76. S. M. Frisch and R. A. Screaton, *Curr. Opin. Cell Biol.*, 2001, **13**, 555-562.
77. L. Li, W. M. Liu, J. C. Wang, Q. Tu, R. Liu and J. Y. Wang, *Electrophoresis*, 2010, **31**, 3159-3166.
78. D. E. Campton, A. B. Ramirez, J. J. Nordberg, N. Drovetto, A. C. Clein, P. Varshavskaya, B. H. Friemel, S. Quarre, A. Breman, M. Dorschner, S. Blau, C. A. Blau, D. E. Sabath, J. L. Stilwell and E. P. Kaldjian, *BMC Cancer*, 2015, **15**.